Accurate Experimental Electronic Properties of DL-Proline Monohydrate Obtained Within 1 Day

T. Koritsánszky, R. Flaig, D. Zobel, H.-G. Krane,
W. Morgenroth, P. Luger*

A 1-day x-ray diffraction experiment on DL-proline monohydrate was performed at 100 kelvin with synchrotron radiation and a charge-coupled device area detection technique. The accuracy of the charge density distribution and of the related electronic properties extracted from these data is comparable or even superior to the accuracy obtained from a 6-week experiment on DL-aspartic acid with conventional x-ray diffraction methods. A data acquisition time of 1 day is comparable to the time needed for an ab initio calculation on the isolated molecules. This technique renders larger molecular systems of biological importance accessible to charge density experiments.

The paramount importance of a charge density distribution $\rho(\mathbf{r})$ (where $\mathbf{r}$ is a vector in crystal space) lies in the fact that all structural elements of an electronic system can be derived from its topology (*1*). On the basis of this physical observable, the theory of "atoms in molecules" provides an atomic partitioning of the molecule and leads to the quantum definition of molecular functional groups. Properties directly deducible from $\rho(\mathbf{r})$, such as the electrostatic potential (EP), can provide information on how molecules might react and how to "design" them for specific applications (*2*). This function is widely used in molecular modeling and design because the chemical and biological functionality of a molecule is closely related to the potential induced by its charge distribution (*3*).

The electron density can be obtained not only by theoretical methods but also by experimental interpretation of single-crystal x-ray diffraction data (*4*). Although this method has been known for more than 30 years (*5*) and many studies have demonstrated its success (*4*, *6*), its wider application has been limited because of complicated and time-consuming experimental requirements. Bragg reflection intensities must be measured at high resolution ($d < 0.5$ Å or $\sin \theta/\lambda > 1.0$ Å^{-1}) (*7*) and at low temperature ($T \sim 100$ K or even lower). Data collection may take several weeks or even months, if the conventional serial data collection technique (with a scintillation counter) is used. The use of area detectors [imaging plates or charge-coupled devices (CCDs)] for small-molecule x-ray work reduces the time requirements substantially (*8*). It is, however, an open debate whether area detectors can provide the sufficiently high-quality data needed for charge density determination.

We report here the collection of an x-ray data set suitable for the charge density determination of DL-proline monohydrate (*9*) (Fig. 1A). The data set was collected at the synchrotron beam line D3 of the storage ring DORISIII at the Hasylab/Deutsches Elektronen-Synchotron, Hamburg. The combination of a primary radiation of wavelength $\lambda = 0.496$ Å (Si monochromator) with a Siemens CCD detector mounted on the detector arm of a Huber four-circle diffractometer allowed the collection of 33,742 Bragg reflections up to $\sin \theta/\lambda = 1.12$ Å^{-1} within 1 day. During the measurement, the temperature of the crystal was maintained at 100 K. The data were reduced to 6758 symmetry-independent reflections, so that roughly four to five observations contributed to each average intensity value. The internal residual, a reliability measure for the agreement of symmetry-related reflections, was 4.3%.

The electron density was represented by the "rigid-pseudoatom" model, as formulated by Hansen and Coppens (*10*), and implemented into the computer program package XD (*11*). In this model, the density deformations, which result from atomic interactions, are described in terms of spherical harmonics multiplied by Slater-type radial functions with energy-optimized exponents (*12*). The expansion was terminated at the hexadecapolar and dipolar level for the heavy and hydrogen atoms, respectively. The unit cell was kept neutral, and no charge transfer was allowed between the water and the proline molecule. The refinement of 309 variables against 5238 observed reflections [$F > 3\sigma(F)$, where $\sigma(F)$ is the standard uncertainty of the structure factor F] yielded a weighted residual R_w of 0.0208, a goodness of fit of 1.35, and a featureless residual $\rho(\mathbf{r})$.

We compared the experimental density and related properties with those obtained theoretically [at the HF/6-311++G(3df,3pd) level] (*13*, *14*) and with those derived by a state-of-the-art conventional diffraction experiment for DL-aspartic acid (*15*) (Fig. 1, A and B). This experiment took more than 6 weeks and resulted in the most extended conventional data set available to date ($\sin \theta/\lambda = 1.37$ Å^{-1}; data were collected at 20 K with Ag Kα radiation and a solid-state detector).

The Laplacian [$\nabla^2\rho(\mathbf{r})$] function maps those regions of space where charge is locally concentrated [$\nabla^2\rho(\mathbf{r}) < 0$] or depleted [$\nabla^2\rho(\mathbf{r}) > 0$] (*1*). The experimental negative Laplacian functions in the plane of the carboxylate groups (Fig. 2, A and B) were used to judge the similarities between the two amino acids and the physical significance of the densities. The relevant features are the bonded valence shell charge concentrations (VSCC) shown by both maps as local maxima in the bonds near the atoms. The nonbonded VSCCs (associated with the lone pair electrons) of the oxygen atoms in proline are more pronounced than those in aspartic acid, an important observation considering the difference in resolution between the two data sets.

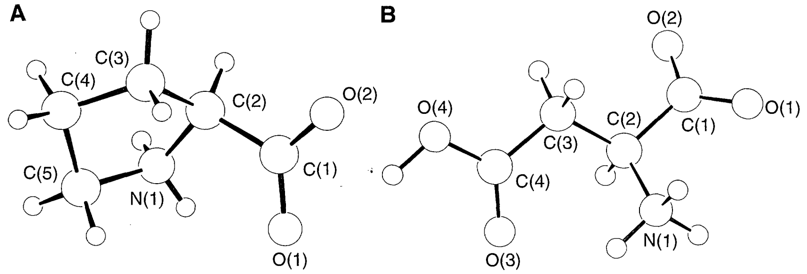

Fig. 1. Graphical representation of proline (**A**) and aspartic acid (**B**) molecules (*19*).

T. Koritsánszky, R. Flaig, D. Zobel, P. Luger, Institute for Crystallography, Free University of Berlin, Takustrasse 6, 14195 Berlin, Germany.
H.-G. Krane, Institute for Mineralogy and Petrography, University of Bonn, Poppelsdorfer Schloss, 53115 Bonn, Germany.
W. Morgenroth, Institute for Mineralogy and Petrography, University of Hamburg, Grindelallee 48, 20146 Hamburg, Germany.

*To whom correspondence should be addressed at luger@chemie.fu-berlin.de

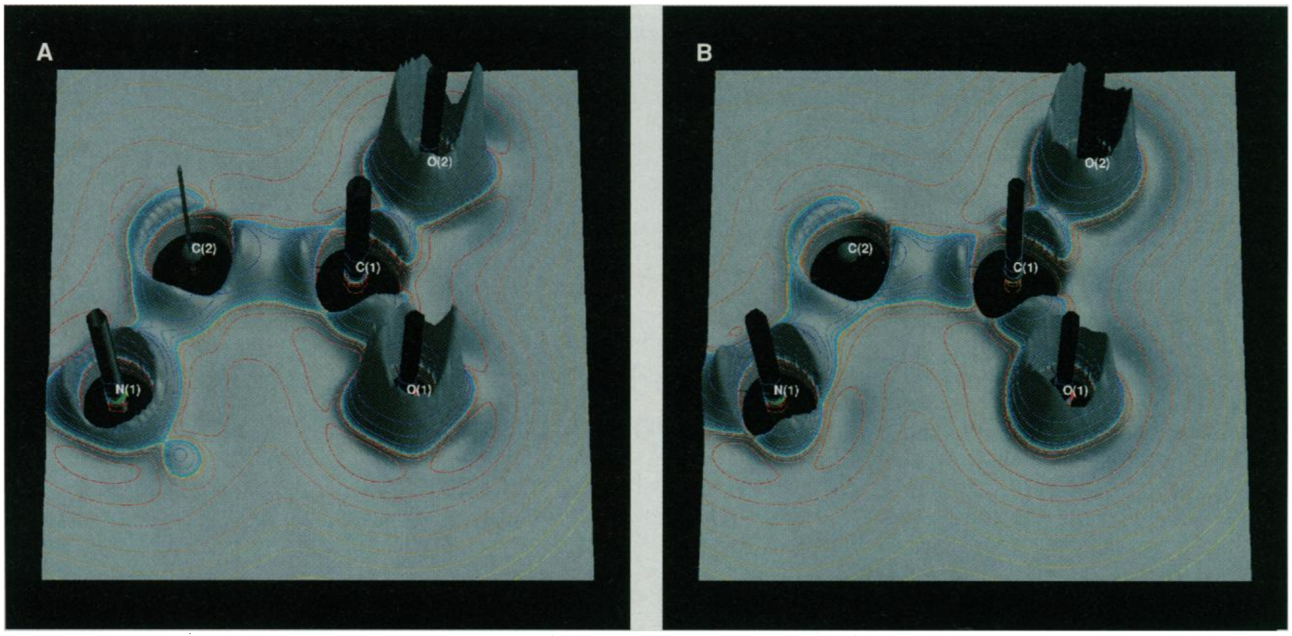

Fig. 2. Relief plots of the experimental negative Laplacian distributions $[-\nabla^2\rho(\mathbf{r})]$ in the planes of the carboxylate groups of DL-proline · H_2O (**A**) and DL-aspartic acid (**B**) for comparison. We generated both maps using the XDGRAPH module of the XD program system (9).

Bond-topological parameters (BTPs) were calculated at the bond critical points (CPs), defined by vectors $\mathbf{r}_b$, where $\nabla\rho(\mathbf{r}_b) = 0$. The BTPs, such as the values of $\rho(\mathbf{r}_b)$ and the Laplacian function $[\nabla^2\rho(\mathbf{r}_b)]$, allow a quantitative comparison of atomic interactions in the two compounds. Experimental BTPs were obtained for both substances, and theoretical BTPs were calculated for proline at the experimental locations of the bond CPs. There is a fair agreement between theory and experiment (Table 1), especially for the $\rho(\mathbf{r}_b)$ values. The experimental and theoretical values of $\rho(\mathbf{r})$ (0.30/0.28 e/Å^3, where e is the electronic charge) and $\nabla^2\rho(\mathbf{r})$ (4.8/6.0 e/Å^5) at the ring CP indicate that the two methods give basically the same results even in the low-density regions, relatively far away from the nuclei. More importantly, the experimental BTPs of proline are in excellent accord with those found for analogous bonds in aspartic acid.

The dipole moment of the proline molecule, calculated from the monopole and dipole populations, is 13.0 D (the Debye unit D = 3.336 × 10^{-30} C · m), which is in good agreement with the value of 12.1 D obtained by a measurement in aqueous solution (16). We calculated the EP from the multipole model density, using the method of Su and Coppens (17), which permits the correct evaluation of this function at any point. Isopotential maps are displayed in Fig. 3, A and B. The dominant feature of the two potential maps is the continuous electronegative region around the carboxylate group, which is found to be more extended on the experimental than on the theoretical EP map. We also observed a similar polariza-

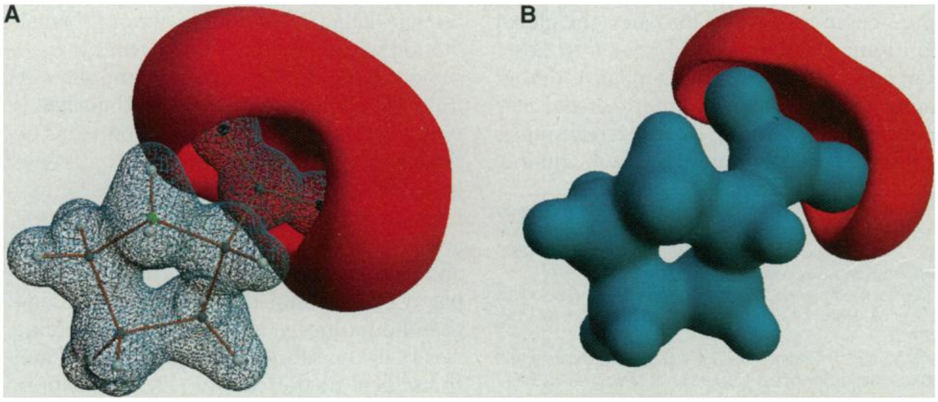

Fig. 3. Three-dimensional isosurface representation of the experimental (**A**) and theoretical (**B**) electrostatic potential of the proline molecule. Surfaces are drawn at constant positive and negative potentials of 0.6 e/Å (blue) and −0.2 e/Å (red). The experimental map (A) is based on the monomolecular density isolated from the crystal structure. This potential unit, together with the EP of the water molecule, is the building block of the crystal's electrostatic potential. Its comparison with the EP of the isolated molecule, derived from ab initio calculation (B), reveals polarization effects caused by the crystal field. We generated both maps using the XDGRAPH module of the XD program system (9).

Table 1. Topological parameters of bonds formed by nonhydrogen atoms. The first and second lines in each set refer to theoretical [HF/6-311++G(3df,3pd)] and experimental values for DL-proline · H_2O; the third line gives experimental values for DL-aspartic acid. The numbers in parentheses indicate the errors in the last digit.

Bond	ρ (e/Å^3)	$\nabla^2\rho$ (e/Å^5)
O(1)–C(1)	2.65	−31.6
	2.83(4)	−39.3(3)
	2.71(3)	−37.6(2)
O(2)–C(1)	2.77	−33.6
	2.84(4)	−34.3(3)
	2.87(3)	−36.1(2)
N(1)–C(2)	1.65	−13.3
	1.68(2)	−9.7(1)
	1.69(2)	−12.9(1)
N(1)–C(5)	1.77	−14.1
	1.70(2)	−8.1(1)
C(1)–C(2)	1.82	−18.9
	1.88(2)	−15.5(1)
	1.69(2)	−12.9(1)
C(2)–C(3)	1.68	−15.7
	1.66(2)	−11.5(1)
	1.61(2)	−12.1(1)
C(3)–C(4)	1.71	−16.1
	1.65(2)	−12.1(1)
C(4)–C(5)	1.77	−17.3
	1.76(2)	−16.1(1)

tion for aspartic acid and attributed it to the effect of hydrogen bonds present in the crystal.

Our diffraction experiment results demonstrate that the combination of synchrotron primary radiation at a wavelength around $\lambda = 0.5$ Å with a CCD area detector can provide a high-precision data set, suitable for accurate charge density determination in a few hours. The results obtained are comparable or even superior to those typically derivable from serial counter data. The short acquisition times open new perspectives for the application of the method on larger molecules of biological importance. In such cases, although the number of reflections increases drastically, there is almost no increase in the measuring time, if an area detector is used. Although the experimental conditions are not yet at an optimum, in the near future, the problems associated with the studies of large systems might be limited to the crystal size and quality rather than to the measuring time. Further improvements can be expected not only from developments in the intensity integration and data-processing strategies of the area detectors (*18*) but also from the intensity increase of synchrotron radiation sources in the next generation.

REFERENCES AND NOTES

1. R. F. W. Bader, *Atoms in Molecules, A Quantum Theory* (Clarendon, Oxford, 1990); R. F. W. Bader, P. Lode, A. Popelier, T. A. Keith, *Angew. Chem.* **106**, 647 (1994).
2. P. Politzer and D. G. Truhlar, *Chemical Applications of Atomic and Molecular Electrostatic Potentials* (Plenum, New York, 1981).
3. B. M. Craven and P. Benci, *Acta Crystallogr. Sect. B* **37**, 1584 (1981); C. Lecomte, M. Souhassou, N. Ghermani, V. Pichon-Pesme, N. Bouhmaida, *Trans. Am. Crystallogr. Assoc. V* **26**, 55 (1990).
4. P. Coppens, *X-ray Charge Densities and Chemical Bonding* (Oxford Science, Oxford, 1997).
5. P. Coppens, *Science* **158**, 1577 (1967); R. F. Stewart, *J. Chem. Phys.* **51**, 4569 (1969).
6. C. Gatti, R. Bianchi, R. Destro, F. Merati, *J. Mol. Struct. (Theochem.)* **255**, 409 (1992); C. Flensburg, S. Larsen, R. F. Stewart, *J. Phys. Chem.* **99**, 10130 (1995); T. Koritsánszky, J. Buschmann, P. Luger, *ibid.* **100**, 10547 (1996).
7. The resolution of the diffraction experiment is defined by $d = \lambda/2\sin\theta$, where θ is the scattering angle and λ is the wavelength of the radiation.
8. A. Darovsky, R. Bolotovsky, V. Kezerashvili, P. Coppens, *Acta Crystallogr. Sect. A* **52**, C-547 (1996); M. Carducci, R. Bolotovsky, P. Coppens, *ibid.*, p. C-342.
9. DL-Proline, the racemic mixture of the naturally occurring amino acid proline, crystallizes as a monohydrate in an orthorhombic cell. The space group symmetry is *Pbca*, and the unit cell is defined by the lattice constant vectors of length $a = 5.253(3)$ Å, $b = 11.987(5)$ Å, and $c = 19.864(10)$ Å. (The numbers in parentheses refer to errors in the last digit.)
10. N. K. Hansen and P. Coppens, *Acta Crystallogr. Sect. A* **34**, 909 (1978).
11. T. Koritsánszky *et al.*, *XD—A Computer Program Package for Multipole Refinement and Analysis of Electron Densities from Diffraction Data* (User Manual, Free University of Berlin, Berlin, 1995).
12. E. Clementi and C. Roetti, *At. Data Nucl. Data Tables* **14**, 177 (1974).
13. M. J. Frisch *et al.* Gaussian 92/DFT, Revision G.1 (Gaussian Inc., Pittsburgh, PA, 1993).
14. It is an ab initio molecular orbital calculation at the Hartree-Fock level of approximation based on the use of Gaussian basis functions. The 6-311++G(3df,3pd) is a triple-zeta basis set and includes diffuse and high-angular momentum functions. This is the most extended standard basis set available in the Gaussian program system.
15. R. Flaig, T. Koritsánszky, D. Zobel, P. Luger, *J. Am. Chem. Soc.*, in press.
16. G. Khanarian and W. J. Moore, *Aust. J. Chem.* **33**, 1727 (1980).
17. Z. W. Su and P. Coppens, *Acta Crystallogr. Sect. A* **48**, 188 (1992).
18. R. Bolotovsky, M. A. White, A. Darovsky, P. Coppens, *J. Appl. Crystallogr.* **28**, 86 (1995).
19. E. Keller, SCHAKAL88: User manual (University of Freiburg, Freiburg, Germany, 1988).
20. Funded by the Bundesminister für Bildung, Wissenschaft, Forschung und Technologie, Bonn, Germany (grant 05 647KEA1), and by the Fonds der Chemischen Industrie, Frankfurt, Germany. We thank B. Dittrich for preparing crystals suitable for the experiment.

14 October 1997; accepted 2 December 1997

Space Geodetic Observations of Nazca–South America Convergence Across the Central Andes

Edmundo Norabuena, Lisa Leffler-Griffin, Ailin Mao,
Timothy Dixon, Seth Stein,* I. Selwyn Sacks,
Leonidas Ocola, Michael Ellis

Space geodetic data recorded rates and directions of motion across the convergent boundary zone between the oceanic Nazca and continental South American plates in Peru and Bolivia. Roughly half of the overall convergence, about 30 to 40 millimeters per year, accumulated on the locked plate interface and can be released in future earthquakes. About 10 to 15 millimeters per year of crustal shortening occurred inland at the sub-Andean foreland fold and thrust belt, indicating that the Andes are continuing to build. Little (5 to 10 millimeters per year) along-trench motion of coastal forearc slivers was observed, despite the oblique convergence.

The high peaks and volcanoes of the Andes and the great earthquakes along the South American coast are dramatic manifestations of ocean-continent plate convergence because the oceanic Nazca plate subducts beneath South America. Convergence occurs over a 500- to 1000-km-wide boundary zone, within which several styles of deformation play a major role in the evolution of the South American continent (*1*).

We studied this convergence using space-based geodetic techniques: the global positioning system (GPS), Satellite Laser Ranging (SLR), and the Doppler Orbitography and Radiopositioning Integrated Satellite System (DORIS). These techniques combine precise satellite-based timing, ranging, and orbit estimation to measure the positions of geodetic monuments to centimeter or better accuracy, such that measurements over time yield precise relative velocities (*2*).

The total relative plate motion is thought to be partitioned into several components (Fig. 1). Some motion accumulates on locked portions of the plate interface at the trench, causing transient elastic deformation, and is released when the interface ruptures in large thrust earthquakes (*3*). Some motion would be expected to occur by stable sliding at the interface, because the slip rate from large subduction zone earthquakes is typically less than the plate motion (*4*). The Andes and their thick crustal root (*5*) suggest that some of the motion causes permanent deformation through crustal shortening and mountain building. Geological studies and seismicity suggest that the high Altiplano plateau should be largely stable and that shortening by thrust faulting and folding occurs in the sub-Andean foreland fold and thrust belt to the east (*6*, *7*). In addition, because convergence is oblique to the trench through much of the region, some trench-parallel motion of coastal forearc slivers might be expected (*8*).

Using space geodesy, we observed the motion of sites within a section across the plate boundary zone. We used GPS to mon-

E. Norabuena, Instituto Geofisico del Peru, Apartado 3747, Lima 100, Peru, and Rosenstiel School for Marine and Atmospheric Sciences, University of Miami, 4600 Rickenbacker Causeway, Miami, FL 33149, USA.
L. Leffler-Griffin and S. Stein, Department of Geological Sciences, Northwestern University, Evanston, IL 60208, USA.
A. Mao and T. Dixon, Rosenstiel School for Marine and Atmospheric Sciences, University of Miami, 4600 Rickenbacker Causeway, Miami, FL 33149, USA.
I. S. Sacks, Department of Terrestrial Magnetism, Carnegie Institute of Washington, 5241 Broad Branch Road, NW, Washington, DC 20015, USA.
L. Ocola, Instituto Geofisico del Peru, Apartado 3747, Lima 100, Peru.
M. Ellis, Center for Earthquake Research and Information, University of Memphis, TN 38152, USA.

---

*To whom correspondence should be addressed.